



SYNTHESIS AND CHARACTERIZATION OF CALCIUM DEFICIENT HYDROXYAPATITE NANOCRYSTALS

A. Anwer^{*1}, M. Kazmi², Z.A. Khan², K. Shahzad³, S. Hussain⁴

¹Department of Basic Sciences and Humanities, University of Engineering and Technology, KSK Campus, Lahore, Pakistan

²Department of Chemical Engineering, University of Engineering and Technology, KSK Campus, Lahore, Pakistan

³Center for Coal Technology, University of Punjab, Lahore, Pakistan

⁴Chemical Engineering Department, NFC IET Multan, Pakistan

Abstract

Synthetic nanoscale calcium deficient hydroxyapatite (CDHA) particles were synthesized using a co-precipitation technique from aqueous solution of calcium nitrate tetrahydrate and diammonium hydrogen phosphate at pH 8.5 at room temperature. No decomposition of CDHA into other phases was observed till 650°C in air for 1h. The product was evaluated using different techniques such as transmission electron microscopy (TEM), X-ray diffraction analysis (XRD), and Fourier transform infrared spectroscopy and Raman spectroscopy. The chemical structural analysis of the obtained product was achieved by using X-ray photoelectron spectrometer (XPS). After heat treatment at 650°C for 1 hour and ageing for 24 h, the product was collected as free flowing white nanopowder with 85% yield.

Keywords: Bioceramics, Calcium Deficient Hydroxyapatite, Nanorods, Bone Regeneration, X-Ray Diffraction.

1. Introduction

During the last few decades, considerable attention has been focused on the synthesis of various nanoceramic biomaterials for biological applications. Among others, calcium phosphate (CaP) bioceramics are well recognized for their use in bone repair applications for use as bulk defect fillers, injectables, the hard phase of biocomposites and coatings on implants because of their excellent biocompatibility and osteoconductivity. There are several kinds of CaP structures which characteristically form a class of compounds named as 'apatites'[1]. The common formula $\text{Ca}_{10-x}(\text{HPO}_4)_x(\text{PO}_4)_{6-x}(\text{OH})_{2-x}$ is for non-stoichiometric apatite, while CaPs have a Ca/P molar ratio in the range of 0.5 $[\text{Ca}(\text{H}_2\text{PO}_4)_2]$ to 2.0 $[\text{Ca}_4(\text{PO}_4)_2\text{O}]$ [2,3].

Hydroxyapatite [HA] is analogous to biological apatite, the principal mineral constituent of teeth and bone and has attracted much attention in orthopaedic science in recent years as a bone replacement and reinforcement material in biomedical composites. because of its biocompatibility, bioactivity and low solubility in wet media. Such nano-bioceramics have

* Corresponding Author: a.anwar@uet.edu.pk

been utilized as a scaffold material to encourage new bone growth for osteographical coatings on metal implants and as a bulk bone fillers [4-7]. Calcium deficient hydroxyapatite, CDHA) has also attracted much attention as component of bone cements; regulating particle properties is frequently used to control cement setting behaviour. CDHA has a high solubility rate in body fluids compared to crystalline stoichiometric HA. Natural bone consists of calcium deficient HA (Ca:P molar ratio less than 1.67) and has a high ion exchange power for numerous cations. In addition, it possessed a very high surface area than pure HA and tricalcium phosphate that could be beneficial for bone replacement applications. The use of CDHA in gas sensing and electrical conductivity makes it a potential candidate [8-9]. Thus, CDHA is extremely useful as an ion-exchange media for the distillation of water and soil contamination with heavy metals [10-14].

Multiple techniques have been used for the synthesis of CDHA. The most common methods are wet precipitation process, microwave synthesis and continuous hydrothermal flow synthesis [15-19]. The major aim of this study is to synthesize crystalline and phase pure CDHA nanopowder using coprecipitation method and to improve the physical and chemical properties of the synthesized materials for better biomedical applications.

2. Materials and Methods

2.1. Chemicals

Calcium nitrate tetrahydrate [$\text{Ca}(\text{NO}_3)_2 \cdot 4\text{H}_2\text{O}$, 99%] Alpha and diammonium hydrogen phosphate [$(\text{NH}_4)_2\text{HPO}_4$, 98%] were purchased from Alpha Aesar, UK. Ammonium hydroxide solution (NH_4OH , 28%) was purchased from VWR International Company.

2.2. Synthesis Methods for Nanopowders

2.2.1. Synthesis of Stoichiometric Nano-Hydroxyapatite

Coprecipitation is one of the oldest methods used for the synthesis of HA nanoparticles. These reactions involve a mixture of soluble calcium and phosphorous sources and the addition of base to result in precipitation of crystalline HA. In the experimental process, 0.3 M diammonium hydrogen phosphate solution was added drop wise to 0.5 M calcium nitrate solutions at room temperature by keeping the Ca:P molar ratio 1.67. The pH of the solutions was kept at pH 11 by adding 10.0 ml of ammonium hydroxide solution.

2.2.2. Synthesis of Calcium Deficient Hydroxyapatite

Calcium deficient hydroxyapatite was prepared at room temperature using coprecipitation route. In this process, 0.3 M diammonium hydrogen phosphate solution and 0.48 M calcium nitrate solutions were used by keeping the Ca:P molar ratio: 1.6. The pH of the reaction mixture was kept above pH 8.5. For this purpose, 5.0 mL of ammonium hydroxide solution was added to both calcium nitrate and diammonium hydrogen phosphate solutions, respectively. The resulting suspension was centrifuged, washed and freeze-dried for 24 h under a vacuum of 0.3 Pa. The product obtained was a fine white powder with ~ 80 % yield.

2.3 Characterization

2.3.1. Chemical analysis

Chemical analysis of CDHA sample was done using a Thermo Scientific X-ray photoelectron spectrometer (XPS) with a two chamber vacuum system with maximum power of 72 W. The X-rays were focused at the source in the range of 30–400 μm . The spectra were collected initially using survey scans at 150 eV. The spectral intensity of the Ag 3d 5/2 peak from clean metal sample was >2.5 Mcps at FWHM of 1.0 eV. The XPS spectra were processed using CasaTM software.

2.3.2. Transmission Electron Microscopy

Transmission electron microscopy was used to analyse the particle morphology. A small amount of sample was dispersed in methanol solution and ultrasonicated for two minutes to yield a very dilute suspension and a few drops of the resulting suspension were then deposited on a carbon-coated copper grid. The grid was dried prior to use in a double tilt holder of the TEM. Image J version 5.0 software was used for assessing size of particles.

2.3.3. X-ray Diffraction

Bruker AXS D4 Endeavour diffractometer was used for XRD analysis of all samples. The data was analysed in 2θ range from 5 to 80° with a scanning step of 0.04° and a count time of 2 sec/step using Cu-K α radiations ($\lambda = 1.5406\text{\AA}$). DIFFRAC^{plus} Eva software was used for the phase analysis of the data by spectral matching with standards patterns. The crystallite sizes were calculated by using Debye-Scherrer equation [20].

2.3.4. FTIR Spectroscopy

The chemical structural properties of the nano-HA were probed using a Nicolet 6700 FTIR. The sample was prepared by grinding with KCl and pressing into a transparent disc. The spectra were collected from 400 – 4000 cm^{-1} with a resolution of 4 cm^{-1} . A background spectrum was collected using a carbon black powder.

2.3.5. Raman Spectroscopy

A Confocal Raman DXR Spectrometer was used. The powder Sample was deposited onto 316L stainless steel block using a spatula. 316 L block was wiped clean first using distilled water then acetone prior to sample analysis. The data was collected using 780 nm laser, 10 X Lens with the scan time of 90 seconds for each sample.

3. Results and Discussion

TEM images of the as synthesized powder revealed small agglomerates and average length along the longest axis of each particle was $ca. 120 \pm 20$ nm and 20 ± 5 nm along the smaller axis (200 particles sampled) as seen in Figure 1 (a) and (b). TEM analysis suggested that particles increase in size after heat-treatment as shown in Figure 1 (c) and (d).

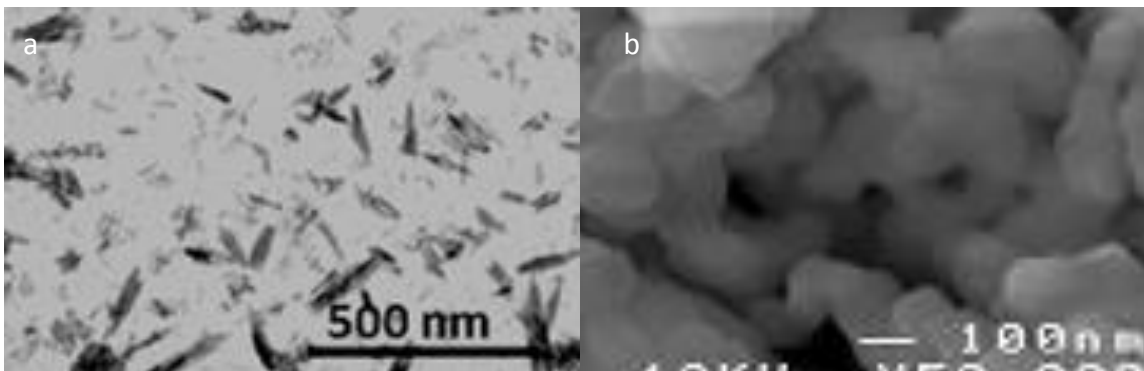


Figure 1. TEM images of as precipitated (a) and heat treated (b) calcium deficient hydroxyapatite samples with scale bars 500 nm and 100 nm, respectively, made via coprecipitation method.

XRD measurements were performed to assess the crystallinity and phase purity of pure HA and CDHA samples. The XRD patterns in all samples confirmed that the samples were crystalline in nature. A broad XRD peak patterns for the as precipitated HA powders suggested an apatite like structure. It was observed that CDHA sample had structural identification with pure HA. While the observed sharp peaks in XRD patterns of the heat- treated HA at 650°C for 1 hour had shown increase in intensity as compared to CDHA as shown in Figure 2.

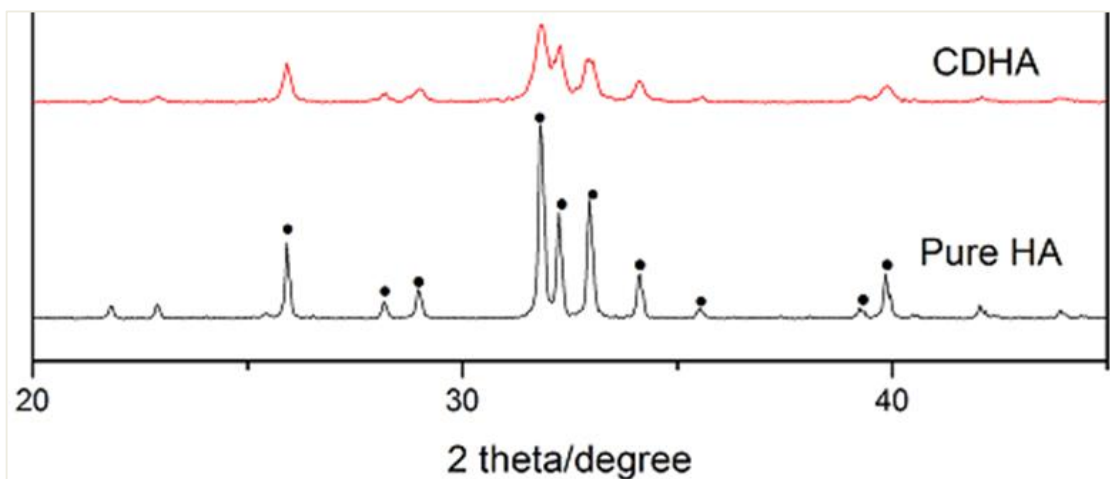


Figure 2. XRD patterns of pure HA and calcium deficient hydroxyapatite samples made via coprecipitation method.

FTIR analysis was used to identify different type of functional groups in calcium phosphates samples [21] as shown in Figure 3. The peaks in FTIR data at 3420 and 632 cm^{-1} corresponded to stretching vibrations of the hydroxyl group in CDHA. Peaks at 1453 and 1414 cm^{-1} corresponded to the stretching mode of vibrations for some carbonate substitutions.

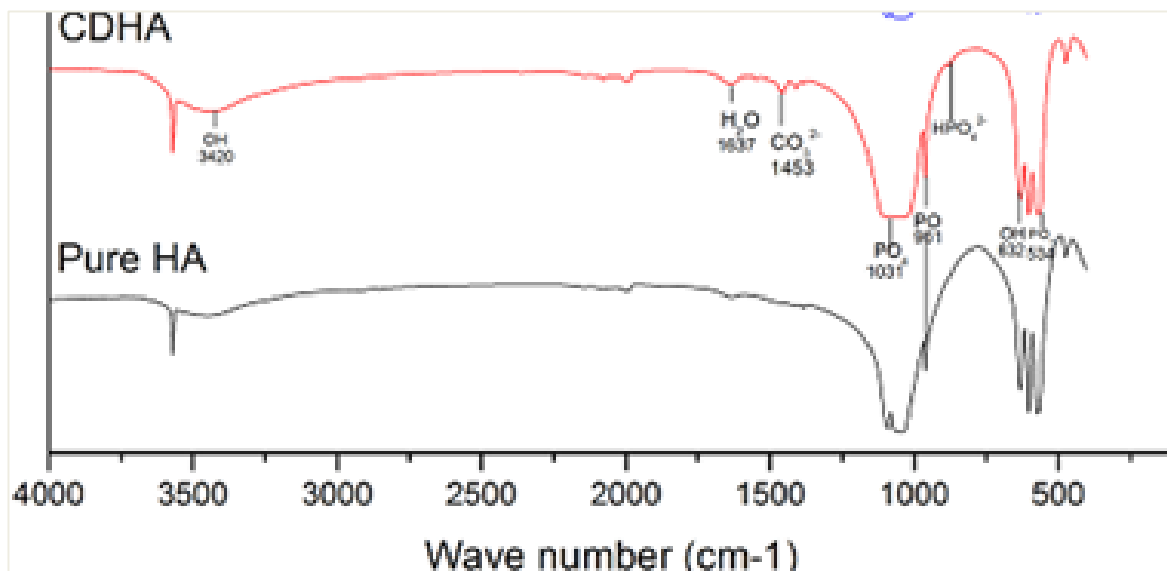


Figure 3. FTIR spectra of pure HA and calcium deficient hydroxyapatite samples made via coprecipitation method.

The absorption peak at 875 cm^{-1} was ascribed to the P–O–H vibration in the HPO_4^{2-} group which confirms the formation of calcium deficient HA [22,23]. Peak at 1031 cm^{-1} corresponds to the P–O asymmetric stretching mode of phosphate, whilst the peaks at 534 and 466 cm^{-1} corresponded to O–P–O linkage.

In order to supplement crystallographic data and detect substitutions in the apatite lattice, raman spectroscopy was performed for both pure HA and CDHA samples. The peak at 965 cm^{-1} corresponded to a symmetric stretching mode of the P–O bands in phosphate [24]. Peaks at 610 and 483 cm^{-1} are likely corresponded to the bending mode of the O–P–O linkage in phosphate as in Figure 4.

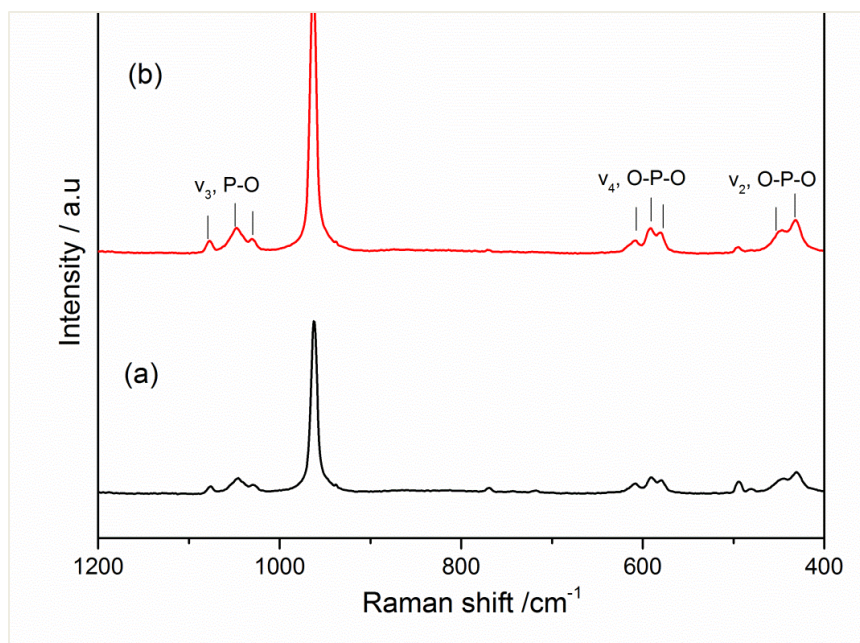


Figure 4. Raman spectra of pure HA and calcium deficient hydroxyapatite samples made via coprecipitation method.

A chemical analysis of CDHA sample was performed by using XPS analysis. The XPS survey spectrum of calcium deficient HA is shown in Figure 5. A small C 1s peak was also observed along with the expected Ca, P and O peaks, which was due to carbon tape used for all analysis. The peaks at 134 eV corresponded to P 2p spectra of hydroxyapatite. The binding energy values for O 1s and Ca 2p were measured as 532 and 347 eV, respectively [25,26]. The Ca/P elemental ratio in the analysed sample was similar to the expected value of 1.5.

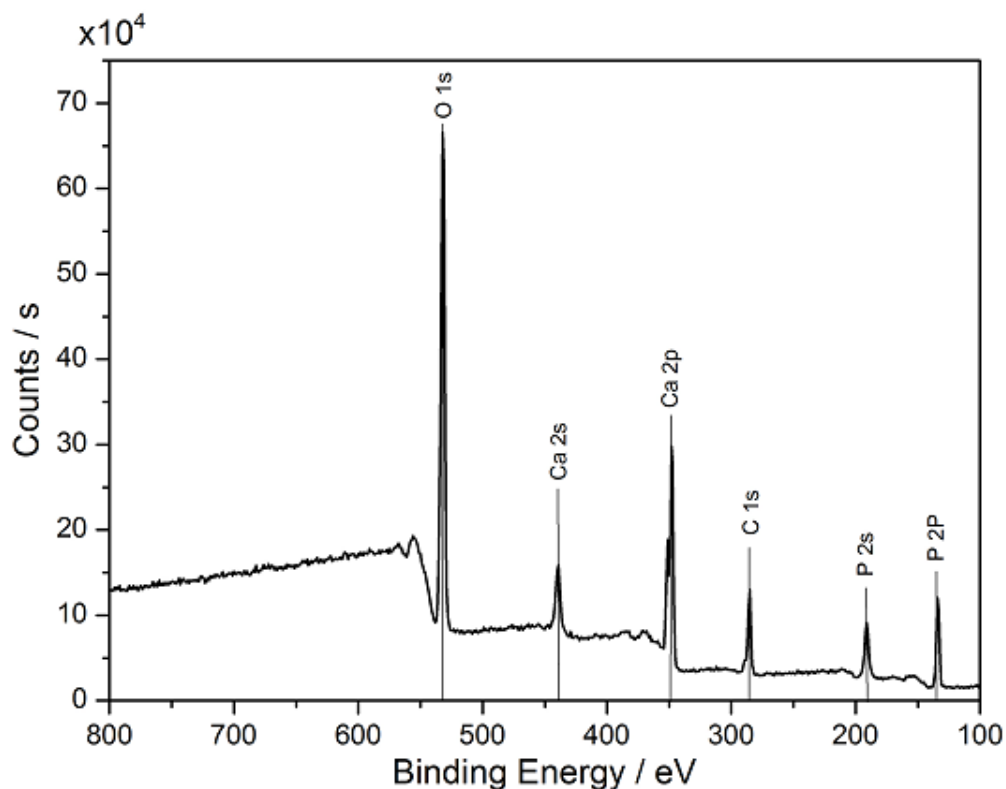


Figure 5. XPS survey spectrum of calcium deficient HA

4. Conclusions

In summary, coprecipitation reactions were successful in synthesizing stoichiometric HA and calcium deficient HA from calcium ion $[\text{Ca}(\text{NO}_3)_2 \cdot 4\text{H}_2\text{O}]$ and phosphate ion source $[(\text{NH}_4)_2\text{HPO}_4]$ as starting material at room temperature. Hence the current work deals with the preparation of synthetic calcium phosphates with optimal properties closer to natural materials (bone and teeth) for use as nanopowders in various biomedical applications.

References

1. J.C. Elliot, Structure and chemistry of the apatites and other calcium orthophosphates. Amsterdam: Elsevier; 1994.
2. L. Hench, J. Wilson, (1993) "An Introduction to Bioceramics" Advanced Series in Ceramics-Vol.1, World Scientific Publishing.
3. L. Hench, The challenge of orthopaedic materials. Current orthopaedics. 2000;14:7-15.

4. B. Kundu, C. Soundrapandian, S.K. Nandi, P. Mukherjee, N. Dandapat, S. Roy, B.K. Datta, T.K. Mandal, D. Basu, R.N. Bhattacharya, Development of new localized drug delivery system based on ceftriaxone-sulbactam composite drug impregnated porous hydroxylapatite: a systematic approach for *in vitro* and *in vivo* animal trial. *Pharm. Res.* 2010, 27, 1659–1676
5. B. Kundu, A. Lemos, C. Soundrapandian, P.S. Sen, S. Datta, J.M.F. Ferreira, D. Basu, Development of porous HAP and β -TCP scaffolds by starch consolidation with foaming method and drug-chitosan bilayered scaffold based drug delivery system. *J. Mater. Sci. Mater. Med.* 2010, 21, 2955–2969.
6. L. Hench, Bioceramics: from concept to clinic. *American Ceramic Society Bulletin.* 1993;72:93-8.
7. A. Afshar, M. Ghorbani, N. Ehsani, M.R. Saeri, C.C. Sorrell, (2003). Some Important Factors in the Wet Precipitation Process of Hydroxyapatite. *Materials & Design*, 24, 197.
8. P. Kasten, R. Luginbuhl, V. Griensven, Barkhausen, C. Krettek, M. Bohner, U. Bosch, *Biomaterials*, Vol. 24,2593 (2003).
9. M.A. Verges, C.F. Gonzalez, M.M. Gallego, J.D. Soolier, Cachadina, E. Matijevic, *J Mater. Res.* Vol. 15, 2526, (2000).
10. R.Z. Legeros, J.P. Legeros, G. Daculsi, R. Kijkowska, *Encyclopedic handbook of biomaterials and bioengineering*, vol2. (New York: Markel Dekker, 1995), 1429-63, Part A.
11. L. Hench, *Bioceramics. J. Am. Ceram. Soc.*, 1998, 81, 1705–1728.
12. S. Kannan, I.A.F. Lemos, J.H.G. Rocha, J.M.F. Ferreira, *Journal of Solid State Chemistry*, 2005, 178, 3190.
13. K. Yoshida, N. Kondo, H. Kita, M. Mitamura, K. Hashimoto, Y. Toda, *Journal of the American Ceramic Society*, 20088, 2315.
14. S. Kannan, J.M.F. Ferreira, *Chemistry of Materials*, 2006, 18,198.
15. A. Mortier, J. Lemaitre, L. Rodrique, P.G. Rouxhet, *J. Solid State Chem*, Vol. 78, 215 (1989).
16. A. Mortier, J. Lemaitre, P.G. Rouxhet, *Thermochimica Acta*, Vol. 143, 265 (1989).
17. M.A. Verges, C.F. Gonzalez, M.M. Gallego, *J. Eur. Ceram. Soc.*, Vol. 18,1245 (1998).
18. A. Siddharthan, S. Seshadri, T.S. Kumar, Rapid synthesis of calcium deficient hydroxyapatite nanoparticles by microwave irradiation. *Trends Biomater Artif Organs.* 2005;18(2):110-3.
19. A.A. Chaudhry, S. Haque, S. Kellici, P. Boldrin, I. Rehman, F.A. Khalid, Instant nano-hydroxyapatite: a continuous and rapid hydrothermal synthesis. *Chemical communications.* 2006(21):2286-8.
20. P. Atkins, J.D. Atkins' *physical chemistry, The investigation of structure.* 2010; 9:699-708.
21. A. Mortier, J. Lemaitre, L. Rodrique, P.G. Rouxhet, *J. Solid State Chem*, 1989; 78: 215-221.

22. A. Mortier, J. Lemaitre, P.G. Rouxhet, *Thermochimica Acta*, Vol. 143, 265 (1989).
23. I. Gibson, I. Rehman, S. Best, W. Bonfield, Characterization of the transformation from calcium-deficient apatite to β -tricalcium phosphate. *Journal of materials science: materials in medicine* 2000; 11:799-804.
24. I. Rehman, M. Karsh, L. Hench, W. Bonfield, Analysis of apatite layers on glass-ceramic particulate using FTIR and FT-Raman spectroscopy. *Journal of biomedical materials research* 2000; 50:97-100.
25. A. Costescu, I. Pasuk, F. Ungureanu, A. Dinischiotu, M. Costache, F. Huneau, Physico-chemical properties of nano-sized hexagonal hydroxyapatite powder synthesized by sol-gel. *Digest Journal of Nanomaterials and Biostructures* 2010; 5:989-1000.
26. H.B. Lu, C.T. Campbell, D.J. Graham, B.D. Ratner, Surface characterization of hydroxyapatite and related calcium phosphates by XPS and TOF-SIMS. *Analytical chemistry* 2000; 72:2886-94.